PB80-181910

Total Particulate Mass Emission Sampling Errors

TRW Systems and Energy
Redondo Beach, CA

Prepared for

Industrial Environmental Research Lab.
Research Triangle Park, NC

Jul 79

U.S. Department of Commerce
National Technical Information Service
NTIS

United States
Environmental Protection
Agency

Industrial Environmental Research
Laboratory
Research Triangle Park NC 27711

EPA-600/7-79-155
July 1979

PB80-181910

EPA

Total Particulate Mass Emission Sampling Errors

Interagency Energy/Environment R&D Program Report

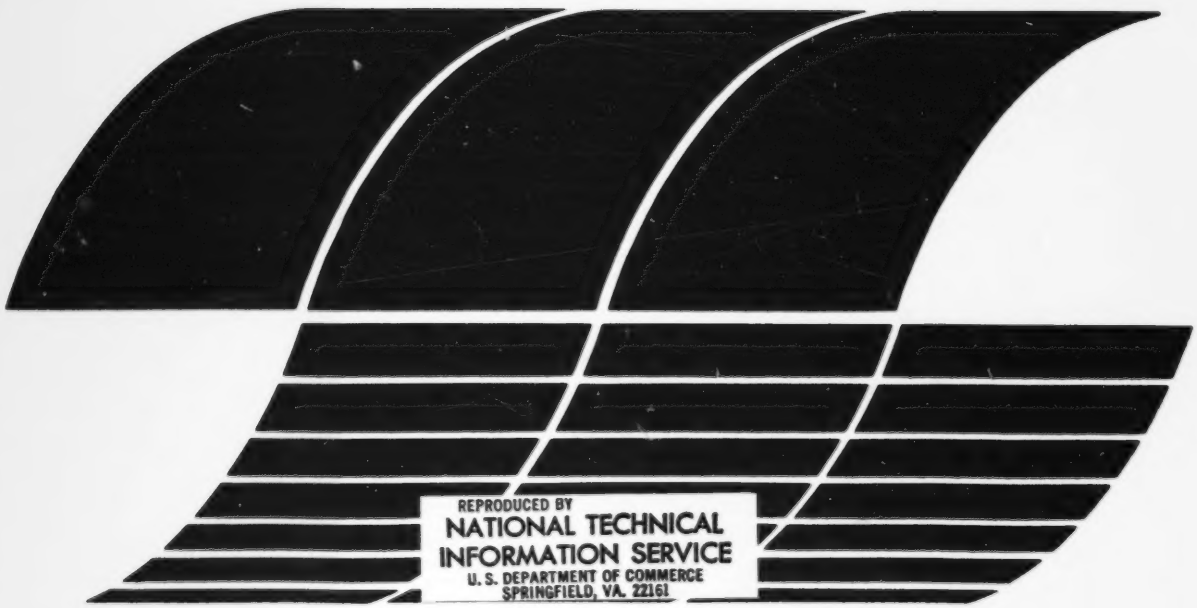

RESEARCH REPORTING SERIES

Research reports of the Office of Research and Development, U.S. Environmental Protection Agency, have been grouped into nine series. These nine broad categories were established to facilitate further development and application of environmental technology. Elimination of traditional grouping was consciously planned to foster technology transfer and a maximum interface in related fields. The nine series are:

1. Environmental Health Effects Research
2. Environmental Protection Technology
3. Ecological Research
4. Environmental Monitoring
5. Socioeconomic Environmental Studies
6. Scientific and Technical Assessment Reports (STAR)
7. Interagency Energy-Environment Research and Development
8. "Special" Reports
9. Miscellaneous Reports

This report has been assigned to the INTERAGENCY ENERGY-ENVIRONMENT RESEARCH AND DEVELOPMENT series. Reports in this series result from the effort funded under the 17-agency Federal Energy/Environment Research and Development Program. These studies relate to EPA's mission to protect the public health and welfare from adverse effects of pollutants associated with energy systems. The goal of the Program is to assure the rapid development of domestic energy supplies in an environmentally-compatible manner by providing the necessary environmental data and control technology. Investigations include analyses of the transport of energy-related pollutants and their health and ecological effects; assessments of, and development of, control technologies for energy systems; and integrated assessments of a wide range of energy-related environmental issues.

EPA REVIEW NOTICE

This report has been reviewed by the participating Federal Agencies, and approved for publication. Approval does not signify that the contents necessarily reflect the views and policies of the Government, nor does mention of trade names or commercial products constitute endorsement or recommendation for use.

This document is available to the public through the National Technical Information Service, Springfield, Virginia 22161.

TECHNICAL REPORT DATA
(Please read Instructions on the reverse before completing)

1. REPORT NO.	2.	3. RECIPIENT'S ACCESSION NO.
EPA-600/7-79-155		PB 80 181910

4. TITLE AND SUBTITLE	5. REPORT DATE
Total Particulate Mass Emission Sampling Errors	July 1979
	6. PERFORMING ORGANIZATION CODE

7. AUTHOR(S)	8. PERFORMING ORGANIZATION REPORT NO.
E. F. Brooks	

9. PERFORMING ORGANIZATION NAME AND ADDRESS	10. PROGRAM ELEMENT NO.
TRW Systems and Energy One Space Park Redondo Beach, California 90278	INE624
	11. CONTRACT/GRANT NO.
	68-02-2165, Task 104

12. SPONSORING AGENCY NAME AND ADDRESS	13. TYPE OF REPORT AND PERIOD COVERED
EPA, Office of Research and Development Industrial Environmental Research Laboratory Research Triangle Park, NC 27711	Task Final; 11/76 - 4/77
	14. SPONSORING AGENCY CODE
	EPA/600/13

15. SUPPLEMENTARY NOTES EPA project officer R. M. Statnick is no longer with IERL-RTP; for details, contact F. E. Briden, Mail Drop 62, 919/541-2557.

16. ABSTRACT The report gives a first-cut estimate of sampling errors in the measurement of total particulate mass emissions from stationary sources. IERL-RTP Procedures Manual: Level 1 Environmental Assessment expresses the desire to measure at accuracies within a factor of + or - 2 to 3. Measurement errors are divided into two general categories: sampling errors and analysis errors. The report deals with evaluation of total particulate mass sampling errors, within the framework of a system error analysis. A mass transport expression is developed in terms of measured parameters to serve as the basis for the analysis. A standard explicit error analysis is performed on the derived expression for mass transport. Since there are also important non-explicit error sources, terms are added to the explicit equation to handle them. The individual error terms are then evaluated on the basis of previous analyses, available empirical data and, where no data are available, estimates. The evaluation leads to a ranking of individual error sources and estimates of total system error. Analysis results show that a Level 1 should have a sampling accuracy of better than a factor of + or -2, with a confidence of 95%, except at a control device outlet where the accuracy is more likely to be a factor of + or -3, especially if the control device is an electrostatic precipitator.

17. KEY WORDS AND DOCUMENT ANALYSIS

a. DESCRIPTORS	b. IDENTIFIERS/OPEN ENDED TERMS	c. COSATI Field/Group
Pollution	Pollution Control	13B
Dust	Stationary Sources	11G
Emission	Particulates	14B
Sampling	Mass Emissions	
Analyzing		
Error Analysis		12A

18. DISTRIBUTION STATEMENT	19. SECURITY CLASS *(This Report)*	21. NO. OF PAGES
Release to Public	Unclassified	
	20. SECURITY CLASS *(This page)*	22. PRICE
	Unclassified	

EPA Form 2220-1 (9-73)

EPA-600/7-79-155

July 1979

Total Particulate Mass Emission Sampling Errors

by

E. F. Brooks

TRW Systems and Energy
One Space Park
Redondo Beach, California 90278

Contract No. 68-02-2165
Task No.104
Program Element No. INE624

EPA Project Officer: Robert M. Statnick

Industrial Environmental Research Laboratory
Office of Energy, Minerals, and Industry
Research Triangle Park, NC 27711

Prepared for

U.S. ENVIRONMENTAL PROTECTION AGENCY
Office of Research and Development
Washington, DC 20460

CONTENTS

	Page
Foreword	iii
List of Tables	iv
Sections	
1. Conclusions	1
2. Recommendations	2
3. Introduction	3
4. Particulate Mass Transport	4
5. Error Analysis	6
6. Evaluation of Error Sources	9
7. Summary and Discussion of Results	15
References	17
Glossary	18
Appendices	
A. Derivation of Mass Transport Equations	20
B. Error Source Evaluation	24
C. Comments on Data and Error Analyses	42

FOREWORD

This report is an analysis of sampling errors in the determination of total particulate mass emissions from stationary sources. In particular, it examines the accuracy which is obtainable with EPA-IERL Level 1 assessment procedures and hardware. It was prepared under Task 26 of EPA Contract 68-02-2165, "Sampling and Analysis of 'Reduced' and 'Oxidized' Species in Process Streams".

This work was conducted under the direction of Dr. R. M. Statnick, Environmental Research Center, Research Triangle Park, North Carolina. The Fluid Physics Department and Applied Chemistry Department, Applied Technology Division, TRW Systems and Energy, Redondo Beach, California, were responsible for the work performed on this task. Dr. C. A. Flegal, Applied Chemistry Department, was Program Manager, and the Task Manager was E. F. Brooks. The author wishes to thank Southern Research Institute for stratification background data and discussions on sampling techniques.

List of Tables

		Page
1.	Values for Minor Error Sources	10
2.	Values for Velocity Measurement Parameter Errors	11
3.	Values for Collected Particulate Mass Error	13
4.	Values for Mapping Error	14
5.	Single Point and System Errors for Total Particulate Mass Sampling	15

1. CONCLUSIONS

- Level 1 total particulate mass emission assessments:
  - A SASS train operated in accordance with "IERL-RTP Procedures Manual, Level 1 Environmental Assessment" sampling at a single point will have a sampling accuracy of a factor of ±2 or better in most locations such as stacks or control device inlets. Under worst case conditions, such as at an ESP outlet, it will have an accuracy of about a factor of ±3.
  - The degree of anisokinetic sampling induced by the SASS train design and operation has a negligible effect on system accuracy.
  - In single point sampling, the mapping error (non-representativeness of the selected point) will be the largest individual error in the system.
  - Sampling accuracy using the SASS train could be improved to about ±25% by using a 16 point traverse rather than sampling at a single point.
- General
  - For traverse sampling, the largest individual error will normally be in collected particulate mass, due to anisokinetic sampling and flow/probe misalignment.
  - System accuracies of ±10% to ±16% can be achieved using commercially available equipment and a 16 point traverse. These accuracy levels, while not required for environmental assessmemt, indicate potential accuracies for control device evaluation testing.

2. RECOMMENDATIONS

- The SASS train in its present state is recommended for Level 1 assessment work, using single point sampling. A modified traverse (along a single line) should be considered for places such as ESP outlets to minimize errors due to stratification.
- Additional stratification data should be obtained at sites such as full scale coal fired power plants for the three general types of most important locations: control device inlets, control device outlets, and stacks. Such data should be obtained with a single (or identical) train(s) to isolate the stratification data.
- Development of methodology to optimize single point sampling accuracy through judicious selection of the sampling point should be pursued through analysis of stratification data and proof of principal source testing for proposed techniques.
- There is a need for lightweight, high volumetric flow sampling hardware and associated procedures to perform quick (1-2 hour) surveys to determine particulate stratification in sources so that appropriate techniques can be used for longer term source assessment testing.
- Additional error analysis work should be performed for size fractionating sampling techniques. The present analysis applies only to the total particulate mass determination.
- Although this report does not deal specifically with Method 5 hardware and procedures, results suggest that for hardware of a given accuracy, there will exist specific procedures to optimize system performance (achieve close to maximum accuracy while minimizing manpower requirements and sampling times). Work should be continued to prepare an IERL-RTP Procedures Manual in this area.

3. INTRODUCTION

The purpose of this report is to present a "first cut" estimate of sampling errors in the measurement of total particulate mass emissions from stationary sources. In "IERL-RTP Procedures Manual: Level 1 Environmental Assessment" (Reference 1), the desire is expressed to perform measurements which are accurate "to within a factor of ±2 to 3." Measurement errors are divided into two general categories: sampling errors and analysis errors. This report deals with evaluation of total particulate mass sampling errors, within the framework of a system error analysis. A mass transport expression is developed in terms of measured parameters to serve as the basis for the analysis. A standard explicit error analysis is performed on the derived expression for mass transport. Since there are also important non-explicit error sources, terms are added to the explicit equation to handle them. The individual error terms are then evaluated on the basis of previous analyses, available empirical data, and, where no data are available, guesses. The evaluation leads to a ranking of individual error sources and estimates of total system error.

For single point sampling, which is recommended in Level 1 work, the analysis shows that accuracies within a factor of two to three should normally be achieved. This conclusion is, however, tentative at present due to a shortage of quantitative data on particulate stratification. Results of this study show that particulate stratification causes the greatest individual error in the system. For traverses using sixteen or more sampling points, it can be said with reasonable certainty that the system error should be less than ±25% when proper hardware and techniques are used. For traverses, the largest error will usually be due to velocity measurement and collected mass uncertainties.

Conclusions are that single point sampling will usually be acceptable for a Level 1 assessment, but additional mapping error work is needed to provide better justification. In addition, methodology development should be pursued to optimize single point sampling techniques – the present method of sampling at a point of average velocity is a step in the right direction, but further refinements are needed.

4. PARTICULATE MASS TRANSPORT

For cases of current interest, it is reasonable to describe the flow stream as consisting primarily of a gas, with small amounts of entrained solid and/or liquid aerosol. The mass transport of the gas is given by (Reference 2):

$$\dot{m}_G = \iint_A \rho_G \vec{u}_G \cdot \vec{n} \, dA \qquad (1)$$

where

$\dot{m}_G$ = total gaseous mass flow rate, g/s

ρ_G = local gas density, g/cm^3

$\vec{u}_G$ = local gas velocity vector, m/s

$\vec{n}$ = unit vector normal to measurement plane, dimensionless

A = area of measurement plane, m^2

Aerosol mass transport can be handled in a number of ways. The most exact would be to consider the particles individually, and use statistical methods dealing with single particle mass and velocity. Since the sampling hardware operates on the particle as being entrained in a gas flow, it is most appropriate from an engineering standpoint to use an entrainment model. This allows us to represent aerosol mass transport in a manner analogous to gaseous mass transport:

$$\dot{m}_A = \iint_A C_A \alpha \vec{u}_G \cdot \vec{n} \, dA \qquad (2)$$

where

$\dot{m}_A$ = total aerosol (liquid and solid) mass flow rate, g/s

C_A = local aerosol concentration, g/cm^3

α = correction factor to account for local difference between mass mean aerosol velocity and gas velocity (i.e., particle slip velocity).

Equation (2) can be considered an exact representation of aerosol mass transport if the proper value of α is selected for each application. For particles of diameter 10 microns or less, we can expect $0.99 < \alpha < 1$ in most streams. The correction factor α is more fully discussed in Appendix B.

The transformation of equation (2) into measured engineering parameters is performed in Appendix A. This transformation is needed to perform a meaningful error analysis. We are presently concerned with two cases: single point sampling and traverse sampling. For these cases, the engineering representations are:

Single point:
$$\dot{m}_A = \propto A \frac{m_A}{V_g} k \cos \theta \sqrt{\frac{2\Delta p \; R \; T_\infty}{p_\infty \; \bar{M}}} \tag{3}$$

Traverse:
$$\dot{m}_A = \propto k\sqrt{2R} \frac{A}{N} \sum_{n=1}^{N} \frac{m_{A_n}}{V_{g_n}} \cos \theta_n \sqrt{\frac{\Delta p_n \; T_{\infty n}}{p_{\infty n} \; \bar{M}_n}} \tag{4}$$

where

k = calibration factor for S probe, dimensionless

θ = angle between local velocity vector and the vector normal to the measurement plane

Δp = measured differential pressure, torr

R = universal gas constant, 8314.32 $\frac{g \cdot m^2}{mole \; s^2 \; °K}$

T_∞ = local static temperature, °K

p_∞ = local static pressure, torr

$\bar{M}$ = local average molecular weight (of the gas), g/mole

m_A = mass of collected aerosol, g

V_g = volume of withdrawn gas at stream temperature, pressure and gas composition, cm^3

$( )_n$ = value of parameters at traverse point n

N = total number of traverse points

These relations are in terms of parameters which are measured directly with the sampling hardware or for which values are established through prior calibration or assumption. The forms of the relations, as is shown in the next section, determine the relative contributions of the individual parameters to total system error.

5. ERROR ANALYSIS

The function of this error analysis is to identify individual sources which contribute to total system error, and to quantify their relative contributions to that error. The value of the analysis lies in two areas – the estimate of total error reflects reliability of the data and can be used to accept or reject individual data points; the estimates of individual errors identify leading error sources, thus indicating where resources should be allocated to improve system accuracy.

The following error analysis is carried out under the assumption of a normal distribution of random errors. This assumption will be valid for most, but not all, of the parameters involved. Reference 3, "The Analysis of Physical Measurements" is a recommended text for appropriate background. The logic of the analysis below is identical to that of error analyses for total volumetric flow and gaseous emissions presented in detail in Reference 2. Consider the general relation (Reference 3):

$$G = f\ (H_1,\ H_2,\ H_3\ ---\ H_r) \tag{5}$$

where

G = dependent variable (quantity to be calculated)

H = independent variable (parameter to be measured)

f = functional relationship

Define the error in the measurement of variable H_r as e_r. The standard deviation of the measurement of H_r is then given by

$$\sigma_r^2 = \lim_{N \to \infty} \frac{\sum_{n=1}^{N} e_{r_n}^2}{N-1} \tag{6}$$

where

σ_r = standard deviation of H_r

N = number of measurements

By derivation, the standard deviation of G is then given as

$$\sigma_G^2 = \left(\frac{\partial f}{\partial H_1}\,\sigma_1\right)^2 + \left(\frac{\partial f}{\partial H_2}\,\sigma_2\right)^2 + \text{----} + \left(\frac{\partial f}{\partial H_r}\,\sigma_r\right)^2 \tag{7}$$

For the present case, it is convenient to analyze the single point relation, equation (3), and then generalize to the traverse case.

Applying equation (7) we obtain:

$$\frac{\sigma^2_{\dot{m}_A}}{\dot{m}^2_A} = \frac{\sigma^2_\alpha}{\alpha^2} + \frac{\sigma^2_k}{k^2} + \frac{\sigma^2_A}{A^2} + \frac{\sigma^2_{m_A}}{m^2_A} + \frac{\sigma^2_{V_g}}{V^2_g} + (\tan^2\theta)\,\sigma^2_\theta$$

$$+ \frac{1}{4}\left(\frac{\sigma^2_{\Delta p}}{\Delta p^2} + \frac{\sigma^2_{\bar{M}}}{\bar{M}^2} + \frac{\sigma^2_{p_\infty}}{p^2_\infty} + \frac{\sigma^2_{T_\infty}}{T^2_\infty}\right) \qquad (8)$$

Equation (8) is presented in a non-dimensional form which will allow us to speak of dimensionless errors rather than the actual standard deviations, which are usually dimensional (e.g., we can consider a temperature error $\sigma_{T_\infty}/T_\infty$ in percent rather than σ_{T_∞} in °K).

The individual error terms in equation (8) correspond to errors which will occur at each point in the stream where a sample is obtained. They are explicit errors in that they are due to identifiable performance aspects of the sampling hardware itself. In addition to these error sources there will also be non-explicit errors due to limitations of the methodology employed. Whenever possible, it is desirable to separate hardware errors from methodology errors so that appropriate hardware and technique can be selected separately to achieve optimum accuracy in any given sampling situation. To accomplish this in the present analysis, we will consider the hardware related errors in equation (8) as those which occur at a given point in the stream. Methodology error terms, introduced below, basically deal with distinctions between the sample obtained at a single point or points and the true total particulate mass emission rate. By definition, then, let $\sigma_{\dot{m}_A}$ in equation (8) be the sampling uncertainty occurring at a point in the stream.

$$\sigma_{SPE} \equiv \left|\frac{\sigma_{\dot{m}_A}}{\dot{m}_A}\right| \times 100\% \qquad (9)$$

where

σ_{SPE} = point error, percent

We can then define a system error as

$$\sigma_{SE}^2 = \sigma_{SPE}^2 + \sigma_{ME}^2 + \sigma_{TE}^2 + \sigma_{AE}^2 \qquad (10)$$

where

σ_{SE} = total system uncertainty, percent

σ_{ME} = mapping uncertainty, percent

σ_{TE} = temporal uncertainty, percent

σ_{AE} = assumption uncertainty, percent

Significance of the individual terms is as follows:

σ_{SPE} — as explained above, this represents the system's capability to extract a representative sample at any one point in the stream, and is determined by the accuracy of the hardware.

σ_{ME} — the mapping uncertainty is associated with stratification in the sample plane. If all other errors are zero, σ_{ME} is a measure of how accurately the sample point or points represent the total aerosol emission.

σ_{TE} — temporal uncertainty is that due to changes in stream conditions during the sampling period, and applies to traverses.

σ_{AE} — the assumption error accounts for inaccuracies in the mathematical model used in a given situation. For example, if the temperature is assumed constant during a traverse when in fact it varies by a few percent in the sample plane, the resulting error will show up in σ_{AE} by definition.

σ_{SE} — this represents the total system error, and is the final desired quantity.

Equations (8), (9), and (10) specifically identify thirteen separate error sources which occur during total particulate mass emission sampling. Of the thirteen, ten are hardware related, and three are methodology related. In the following section, the individual terms are quantitatively evaluated and the leading sources of error are specifically identified.

6. EVALUATION OF ERROR SOURCES

This section deals with quantitative evaluation of the thirteen error terms identified in Section 5, with the objective of producing realistic estimates of total system error. Emphasis is placed on a summary of evaluations and comments on leading error sources. A more detailed evaluation of individual terms is presented in Appendix B. Two points should be kept in mind when considering the data presented below: (1) The errors, presented in terms of standard deviations, are random errors, rather than systematic errors due to causes such as instrument calibration shifts or mistakes due to operator error. (2) For normally distributed errors, the standard 95% engineering confidence interval is represented by a $\pm 2\sigma$ interval. Most, but not all, of the errors can be reasonably represented by a normal distribution. For non-normally distributed errors, emphasis is placed on the "95% confidence" aspects rather than on trying to determine the appropriate type of distribution.

Of the thirteen error sources, seven are generally rather small and well understood. These are treated briefly as a group. Following that is commentary on the three terms related to velocity measurement, which are well understood but are not always small. The section concludes with individual discussion of the temporal error, collected particulate mass error, and mapping error.

6.1 Generally Small, Well Understood Error Sources

Errors in static pressure and temperature, duct cross-sectional area, and average molecular weight of the gas are usually small because the parameters are not difficult to measure in most applications. When significant errors do occur, they are usually systematic in nature and are due to such things as improper calibration practices, unaccounted for wall deposits which reduce the flow area, and other procedural errors. The error due to particle slip velocity is typically small due to the particle size distribution and density encountered in most process streams. The slip velocity, represented by α, is treated further in Appendix B. The other terms mentioned above are discussed at length in Reference 2.

The assumption error will be small as long as adequate attention is paid to sampling details. This means that each of the parameters in equation (3) should be measured at each sampling point. The form of equation (3) is sufficiently exact and inclusive that assumption errors will be relatively small. Assumption errors are also treated at greater length in Reference 2.

The error in the volume of withdrawn gas will be small when adequately calibrated equipment is used and it is acknowledged that V_g is based upon stack temperature, pressure, and composition, which usually means that the instrument reading (e.g., from a dry test meter) must be properly corrected for temperature and pressure, and condensible and volatile stream components must be accounted for.

Achievable errors for the above parameters are presented below in Table 1. The listed accuracies are not difficult to obtain with generally available equipment as long as adequate care is taken to avoid systematic errors.

Table 1. Values for Minor Error Sources

Parameter	2σ (95% Confidence Interval) Error, Percent
$\bar{M}$	±2
p_∞	±2
T_∞	±2
A	±2
α	±2
V_g	±2
Assumption Error	±2

6.2 Velocity Measurement Parameter Errors

These are errors associated with the parameters k, θ, and Δp. They are discussed at considerable length in References 2 and 4. Errors for various types of hardware and flow conditions are given in Appendix B, and summarized in Table 2.

Table 2. Values for Velocity Measurement Parameter Errors

Parameter	Related Component	Error
k	Pitot-static probe	$2\frac{\sigma_k}{k} \times 100\% = \pm 0.5\%$
	S-type probe	$2\frac{\sigma_k}{k} \times 100\% = \pm 1\%$
θ		
a. near flow disturbance	Pitot-static	$2(\tan\theta)\,\sigma_\theta \times 100\% = \pm 1.3\%$
	S-type	$2(\tan\theta)\,\sigma_\theta \times 100\% = \pm 8\%$
b. far from flow disturbance	Pitot-static	$2(\tan\theta)\,\sigma_\theta \times 100\% = \pm 0.5\%$
	S-type	$2(\tan\theta)\,\sigma_\theta \times 100\% = \pm 2\%$
Δp	U-tube manometer	$2\sigma_{\Delta p} = \pm 0.065$ Torr
	SASS train[1]	$2\frac{\sigma_{\Delta p}}{\Delta p} \times 100\% = \pm 14\%$[2]
	Baratron	$2\frac{\sigma_{\Delta p}}{\Delta p} \times 100\% = \pm 0.16\%$[3]

[1] Δp read on 0-.5 or 0-4 in H_2O Magnehelic gage

[2] nominal velocity range 6-40 m/s

[3] nominal velocity range 1.7-55 m/s

The SASS train, selected for Level 1 assessments, employs an S-type pitot probe and two Magnehelic differential pressure gages. These components comprise a low cost, reasonable accuracy system. The high accuracy Baratron/pitot-static probe combination has been used in the field by TRW without handling problems (Reference 4), and is recommended, especially for very low flow velocities (< 5 m/s), in situations where accuracy takes precedence over hardware cost.

6.3 Temporal Variation Errors

The temporal error, σ_{TE}, is difficult if not impossible to evaluate when significant changes occur during the period of traverse. The best way to handle the problem is the standard approach of being sure that plant operating conditions are held constant during the sampling period, and discarding the data if they are not. Concurrently, it is also desirable to minimize the sampling time by maximizing the sample flow rate, as is done with the SASS train. The constant attention of the sampling team is required during the sampling period to detect variations in flow or other critical parameters. The estimated value for $2\sigma_{TE}$ in sources such as power plants is ±4%.

6.4 Collected Particulate Mass Errors

The term σ_{m_A} gives the accuracy with which the sampling probe obtains an aerosol sample representative of the point at which the probe is placed. The major error contributions result from anisokinetic sampling and from sample loss or gain within the collection system. Anisokinetic errors, due to improper sampling rate and/or probe misalignment, are treated at length in Appendix B. Sample gain or loss is usually due to improper hardware design or procedures. The appropriateness of condensing some types of vapors and considering the result as particulate is a philosophical battleground which will not be trod upon here. A 2σ error of ±4% in collected mass due to aerosol gain or loss is considered reasonable for a sampling system such as the SASS train.

Isokinetic sampling is achieved for different gas velocities through variation of the sampling rate, the nozzle orifice diameter, or both. Size fractionating devices like the SASS train require a constant, fixed flow rate so that adjustments to approximate isokinecity must be done by varying the nozzle I.D. Nozzle diameters are typically available in .32 cm (.125 in.) intervals, which allows maximum deviation from isokinetic sampling to be calculated, as is done in Appendix B.

The magnitude of achievable isokinetic sampling errors depends on the type of hardware used (e.g., fixed or variable sample rate), component

accuracy, and stream conditions (particle size distribution and local flow direction). Collected mass errors, as determined in Appendix B, are summarized below in Table 3 for several general cases.

Table 3. Values for Collected Particulate Mass Error

Sampling Location	Collected Mass Error, $2\frac{\sigma_{m_A}}{m_A} \times 100\%$	
	SASS Train	Maximum Accuracy Train*
Control device inlet	±20%	±8%
Control device outlet	±16%	±8%
In stack, ≥ 8 diameters above breeching	±10%	±6%

*Hypothetical train using best readily available hardware components.

6.5 Mapping Errors

In the case of single point sampling, which is the method recommended for Level 1 assessments, the mapping error will usually be the largest single error in the system. Consequently, the mapping error deserves considerable attention. The major problem encountered so far has been a shortage of particulate stratification data, which is essential in evaluation of mapping techniques. The bulk of the data examined to date has been comparisons of single point impactor measurements and Method 5 type traverses. Due to significant differences between the types of sampling trains, it is difficult to isolate the differences in output which are due solely to stratification. Data examined and discussion thereof are presented in Appendices B and C, respectively. Mapping error estimates for single point sampling and 16 point traverses are presented in Table 4 for various types of conditions.

Table 4. Values for Mapping Error

Sampling Location	Mapping Error, $2\sigma_{ME}$	
	Single Point	16 Point Traverse
Control device inlet	+60%, -40%	±8%
Control device outlet	+150%, -60%	±12%
In stack, ≥8 diameters above breeching	+50%, -33%	±5%

As Table 4 shows, maximum mapping errors tend to occur at a control device outlet, especially for electrostatic precipitators, meaning that stratification is increased by the control device. Just as it is a general rule for velocity measurement to avoid working immediately downstream of a large flow disturbance, it is wise in particulate sampling to avoid sampling immediately downstream of a stratification source. When sampling is done near such a source, such as an ESP outlet, knowledge of the ductwork and characteristics of the source can be used to select a single sampling point which would be more representative than a randomly selected point.

7. SUMMARY AND DISCUSSION OF RESULTS

Error values in Tables 1-4 were substituted into equations 8-10 to obtain single point and system errors, which are shown in Table 5. The point error, σ_{SPE}, is indicative of hardware accuracy, while the system error, σ_{SE}, indicates the combined hardware and procedure accuracy.

Table 5. Single Point and System Errors for Total Particulate Mass Sampling

Sampling Train	Sampling Location	Error			Largest Error Source	
		$2\sigma_{SPE}$	$2\sigma_{SE}$		Single Point	16 Point
			Single Point	16 Point		
SASS	Control device inlet	±23%	+64%, -46%	±24%	σ_{ME}	σ_{m_A}
	Control device outlet	±20%	+150%, -64%	±24%	σ_{ME}	σ_{m_A}
	Stack, ≥ 8 dia. above breeching	±13%	+52%, -36%	±15%	σ_{ME}	σ_{m_A}
Maximum Accuracy*	Control device inlet	±9%	+60%, -42%	±13%	σ_{ME}	σ_{ME}, σ_{m_A}
	Control device outlet	±9%	+150%, -60%	±16%	σ_{ME}	σ_{ME}
	Stack, ≥ 8 dia. above breeching	±7%	+50%, -34%	±10%	σ_{ME}	σ_{m_A}

*Hypothetical train using best readily available hardware components.

The "Maximum Accuracy" train in Table 5 is a train which would consist of the highest accuracy components readily available commercially. For example, it would include a high accuracy differential pressure transducer. The purpose in showing the "Maximum Accuracy" train error estimates is only to illustrate the best state of the art capabilities.

A comparison of relative accuracies of hardware and procedures is given by σ_{SPE} and σ_{SE}. For single point sampling, σ_{SE} is invariably large compared with σ_{SPE}, due to the single point mapping error. Thus hardware improvements in the SASS train would not improve the system accuracy when single point sampling is used. For traverses, the situation is different. The SASS train system accuracy is limited by the hardware rather than by procedure, while for the Maximum Accuracy train, the respective hardware and procedure errors are about equal.

There has been a twofold reason for performing the above analyses. The first has been to determine whether hardware and procedures recommended for Level 1 assessments are adequate to produce the desired "factor of ± 2 to 3" accuracy. The second has been to determine optimum accuracy capabilities and to show where future efforts should be devoted to optimize system accuracy. Results of the analyses show that a Level 1 assessment should have a sampling accuracy of better than a factor of ± 2 except at a control device outlet, where the accuracy is more likely to be a factor of 3, especially if the control device is an ESP. It is likely true that the error at a control device outlet can be reduced by making use of known device characteristics in selecting a sample point. This type of methodology should be pursued. For very high accuracy work, Table 5 indicates that there is a good match between the accuracies of currently available hardware and traverse sampling procedures. Future work in this area would involve integration of high accuracy components into a viable system for efficient traverse sampling.

In conclusion on the matter of Level 1 assessments, it is recommended that sampling after a control device be done in a stack whenever feasible- rather than directly at the control device outlet. This will be the best way to optimize accuracy. In addition, development of methodology for single point sampling and/or modified traverse sampling (along a single line to minimize moving of equipment) directly at a control device outlet should be pursued to minimize the error due to particulate stratification.

REFERENCES

1. "IERL-RTP Procedures Manual: Level 1 Environmental Assessment," EPA-600/2-76-160a, Hamersma, Reynolds, and Maddalone, June 1976.

2. "Flow and Gas Sampling Manual," EPA-600/2-76-203, Brooks and Williams, July 1976.

3. The Analysis of Physical Measurements, E. Pugh and G. Winslow; Addison-Wesley, 1966.

4. "Continuous Measurement of Total Gas Flowrate from Stationary Sources," EPA-650/2-75-020, Brooks, et al., February 1975.

(See Appendices for additional references.)

GLOSSARY

SYMBOL	USAGE
A	flow cross-sectional area, m^2
C_A	true aerosol concentration in the stream ahead of the probe, g/cm^3
C_m	aerosol concentration inside probe entry, g/cm^3
D_p	particle diameter, cm
D_s	sample probe orifice diameter, cm
f	empirical functional relationship; functional relationship
G	dependent variable (quantity to be calculated)
H	independent variable (parameter to be measured)
k	pitot probe calibration factor, dimensionless
m_A	mass of collected aerosol, g
$\dot{m}_a$	total aerosol (liquid and solid) mass flow rate, g/s
$\dot{m}_G$	total gaseous mass flow rate, g/s
$\overline{M}$	local gas average molecular weight, g/mole
$\vec{n}$	unit vector normal to measurement plane, dimensionless
N	number of measurements; total number of sampling points
p_∞	local static pressure, torr
p_o	local stagnation pressure, torr
Δp	$p_o - p_\infty$, the pressure differential between the local stagnation and static pressures, torr
R	universal gas constant, 8314.32 $\frac{g \cdot m^2}{mole\ S^2\ {}^oK}$
T_∞	local gas static temperature, ^oK
$\vec{u}_G$	local gas velocity vector, m/s
U_G	true gas velocity ahead of the probe, cm/s
U_m	mean velocity at probe inlet, cm/s

SYMBOL	USAGE
V_g	volume of withdrawn gas at stream temperature, pressure, and gas composition, cm^3
$( )_n$	value of parameter at sample point n
α	correction factor to account for local difference between mass mean aerosol velocity and gas veloctity (i.e., particle slip velocity).
β	$\frac{D_p \rho_p U_G}{18\mu D_s}$
θ	angle between local velocity vector and duct axis
μ	gas viscosity, poise
ρ_G	gas density, g/cm^3
ρ_p	particle density, g/cm^3
σ_{AE}	assumption uncertainty, percent
σ_{ME}	mapping uncertainty, percent
σ_{SE}	total system uncertainty, percent
σ_r	standard deviation of H_r
σ_{SPE}	point error, percent
σ_{TE}	temporal uncertainty, percent

APPENDIX A. DERIVATION OF MASS TRANSPORT EQUATIONS

This appendix deals with the transformation of the particulate conservation of mass equation (equation (2) in Section 4) into the engineering representations shown in equations (3) and (4) in Section 4. The conservation of mass equation is:

$$\dot{m}_A = \iint_A C_A \alpha \vec{u}_G \cdot \vec{n} \, dA \qquad \text{(A-1)}$$

where

$\dot{m}_a$ = total aerosol (liquid and solid) mass flow rate, g/s

C_A = local aerosol concentration, g/cm^3

α = Correction factor to account for local difference between mass mean aerosol velocity and gas velocity (i.e., particle slip velocity).

A = flow cross-sectional area, m^2

Equation (A-1) is a convection model which states that the local aerosol concentration is convected downstream with the gas at a speed equal to the gas velocity component in the axial flow direction multiplied by a correction factor α which accounts for inertial and gravitational forces on the particles. As the particle mass to cross-sectional area ratio becomes small, α goes to unity, which represents complete entrainment. As that ratio becomes large, α goes to zero, representing non entrainment. For most processes of interest, α will be very close to unity, and is not measured in practice.

For purposes of the error analysis, we need to take equation (A-1) and put it in terms of actual engineering parameters. In most cases, it is not practical to take the entire gas stream and process it to determine the particulate content. Standard techniques involve obtaining samples from one or more discrete points in the stream. For these two cases, single point and traverse sampling, equation (A-1) becomes

Single point: $\dot{m}_A \approx C_A \propto \vec{u}_G \cdot \vec{n}\, A$ (A-2)

Traverse: $\dot{m}_A \approx \sum_{n=1}^{N} \left(C_{A_n} \propto_n \vec{u}_{G_n} \cdot \vec{n}\right) \Delta A_n$ (A-3)

where

N = total number of sampling points

$( )_n$ = value of parameter at sample point n.

For a typical sampling train, the aerosol concentration is measured as

$$C_A = \frac{m_A}{V_g} \tag{A-4}$$

where

m_A = mass of collected aerosol, g

V_g = volume of withdrawn gas at stream temperature, pressure, and gas composition, cm^3

The aerosol mass m_A is determined by weighing the collected samples, and the gas volume is measured with a dry gas meter or similar device, with correction being made for moisture removed ahead of the meter.

The flow cross-sectional area, A, is usually determined from blueprints, especially in the case of rectangular ducts. For traverses, all common techniques divide the area up into segments of equal size, so that

$$\Delta A_n = \frac{A}{N} \tag{A-5}$$

The axial component of the gas velocity is usually measured by means of a pitot probe and differential pressure device for the primary measurement. The transformation is as follows:

$$\vec{u}_G \cdot \vec{n} = |\vec{u}_G| \cos \theta \tag{A-6}$$

where

θ = angle between local velocity vector and duct axis

For notational simplicity, define

$$u_G \equiv \left|\vec{u}_G\right| \tag{A-7}$$

We will normally be dealing with incompressible gas flows, so that

$$u_G = k\sqrt{\frac{2\Delta p}{\rho_G}} \tag{A-8}$$

where

$\Delta p = p_o - p_\infty$, the pressure differential between the local stagnation and static pressures, torr

ρ_G = gas density, g/cm^3

k = pitot probe calibration factor

Substituting the equation of state,

$$\rho_G = \frac{p_\infty}{\frac{R}{\overline{M}} T_\infty} \tag{A-9}$$

where

p_∞ = local static pressure, torr

R = universal gas constant, 8314.32 $\frac{g \cdot m^2}{mole\ S^2\ {}^oK}$

$\overline{M}$ = local gas average molecular weight, g/mole

T_∞ = local gas static temperature, ${}^oK$

for ρ_G, we obtain

$$\vec{u}_G \cdot \vec{n} = u_G \cos\theta = k(\cos\theta)\sqrt{\frac{2\Delta p\ R\ T_\infty}{p_\infty\ \overline{M}}} \tag{A-10}$$

Substituting into equations (A-2) and (A-3), we obtain

Single point:

$$\dot{m}_A = \propto A \frac{m_A}{V_g} k \cos\theta \sqrt{\frac{2\Delta p\ R\ T_\infty}{p_\infty\ \overline{M}}} \tag{A-11}$$

Traverse:

$$\dot{m}_A = \propto k \sqrt{2R} \frac{A}{N} \sum_{n=1}^{N} \frac{m_{A_n}}{V_{g_n}} \cos \theta_n \sqrt{\frac{\Delta p_n \, T_{\infty n}}{p_{\infty n} \, \overline{M}_n}} \qquad \text{(A-12)}$$

The conservation of mass equation is now presented in terms of normal engineering parameters. Of the terms in equations (A-11) and (A-12), the following are usually measured directly with sample train components and support equipment: m_A, V_g, Δp, T_∞. The area A is either measured or determined from blueprints. The static pressure p_∞ is often determined by adding (or subtracting, as required) the differential pressure between the stream pressure and ambient pressure to barometric pressure, which is usually available. The average molecular weight, $\overline{M}$, is either measured or estimated from plant operating conditions. The pitot probe calibration constant should be determined by pre- and post-test calibration. The slip velocity factor $\propto$ is usually ignored (therefore considered to be unity). Flow angularity is also typically ignored, meaning $\cos \theta = 1$, but it is possible to use a velocity probe which automatically compensates for angularities up to 30°, as is discussed in Appendix B. Equations (A-11) and (A-12), which appear as equations (3) and (4) in Section 4, serve as the basis for the error analysis in Section 5.

APPENDIX B. ERROR SOURCE EVALUATION

The purpose of this appendix is to provide background to support the summaries of evaluations presented in Section 6. Emphasis here will be placed on understanding the physics of some of the key parameters, and on presentation of empirical data, in particular for stratification. Emphasis is placed on three areas: velocity measurement, collected particulate mass, and stratification.

1. Particle Slip Velocity Factor

Of the "generally small, well understood error sources", only the slip velocity factor α warrants additional treatment here. Particle velocities will differ from the gas velocity due to gravity forces and inertial forces, the latter arising when there is a change in flow direction. The magnitude of the particle/gas velocity differential is most easily illustrated for the case of a flow going directly up a vertical stack. In this situation, gravity produces a downward force which makes the particle velocity less than the gas velocity. The result is a local Stokes flow condition in which the differential velocity is identified as the settling velocity of the particles. Settling velocity is plotted in Figure B-1 as a function of particle size (spherical particles) for two different values of particle density and gas viscosity. The slip velocity factor would then be calculated from the particle settling (terminal) velocity and the gas velocity. As Figure B-1 shows, the settling velocity will be at most a few centimeters/second for particles smaller than 10 microns. A vertical flow represents the worst case in terms of gravitational effects. Inertial effects can usually be ignored due to the velocities involved. It typically takes a special effort, as in the case of cyclones and impactors, to produce the high velocities and sharp turning angles required to make inertial effects important.

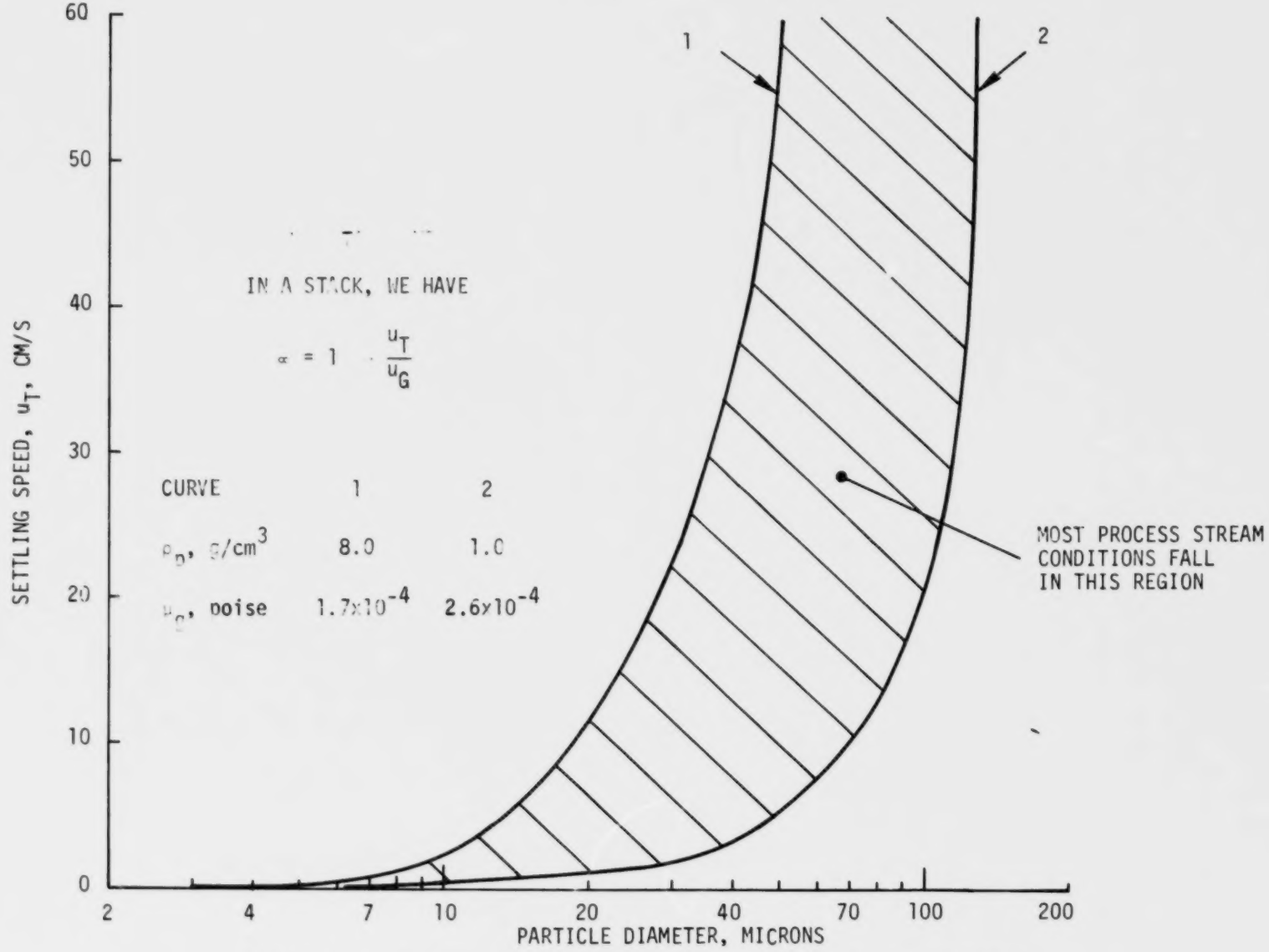

Figure B-1. Settling speed of spherical particles in a combustion stream as a function of particle size

2. Gas Velocity Measurement

Present concern is limited to measurement techniques involving a pitot probe and differential pressure measurement device. The most common types of pitot probes are the S-type probe typically used in field testing, and the pitot-static probe, which has tended to acquire a reputation of being acceptable for use only in the laboratory. The 2σ calibration factor accuracies of $\pm$ .5% and $\pm$ 1% for the pitot-static probe and S probe, respectively, shown in Table 2 in the main text were obtained from References B-1 and B-2. Angularity sensitivity data in Table 2 were obtained from the same sources. The data are shown in Table B-1 below.

Table B-1. Errors due to Flow Angularity for S-Type and Pitot-Static Probes

Flow Angularity	2σ Velocity Error, 2 (tan θ) σ_θx100%	
	"S" Pitot Probe	Pitot Static Probe
yaw, degrees		
± 5	+1.6	+0.3
±10	+3.5	+1.0
±20	+4.5	+1.3
±30	+7.5	+0.2
pitch, degrees		
+ 5	+1.5	+0.3
+10	+2.0	+1.0
+20	+3.5	+1.3
+30	+4.5	+0.2
- 5	-1.5	+0.3
-10	-2.5	+1.0
-20	-5.0	+1.3
-30	-8.0	+0.2

For the "near flow disturbance" case in Table 2, a flow angularity range of $\pm 30^{o}$ was assumed, while the range was selected to be $\pm 5^{o}$ for the "far from flow disturbance" case. As the data show, the pitot static probe has the more desirable characteristics.

Accuracy of differential pressure measurement devices is presented in Figure B-2. The zig-zag in the SASS train curve corresponds to a switch from the low range to the high range Magnehelic gage. Summary data in Table 2 were taken from this plot.

3. Collected Particulate Mass

The Level 1 particulate collection procedure has been questioned (Reference B-3) for single point sampling and for not sampling in a strictly isokinetic manner. The isokinetic problem is addressed here, while single point sampling (mapping) errors are discussed in the following section.

The term σ_{m_A} gives the accuracy with which the sampling probe obtains an aerosol sample representative of the point at which the probe is placed. The major contributions to error come from anisokinetic sampling and from sample loss or gain within the probe. Loss of sample could occur due to poor system design or procedural errors, while sample gain is due to vapor condensation, which would also be hardware and/or procedure related. Sample alteration should not be a major problem in a properly designed and operated system.

Isokinetic sampling errors will occur in even the most careful work due to equipment random errors and stream conditions. Some general comments about the concept of isokinetic sampling are in order here. Textbook explanations of isokinetic sampling show smooth streamlines in the flow around the sample probe inlet, with streamline deviations illustrating anisokinetic conditions. In reality, such a situation exists only in steady laminar flows, as can be produced in a good wind tunnel. Laminar flows will not be encountered in the field. In steady, laminar flows, streamlines are

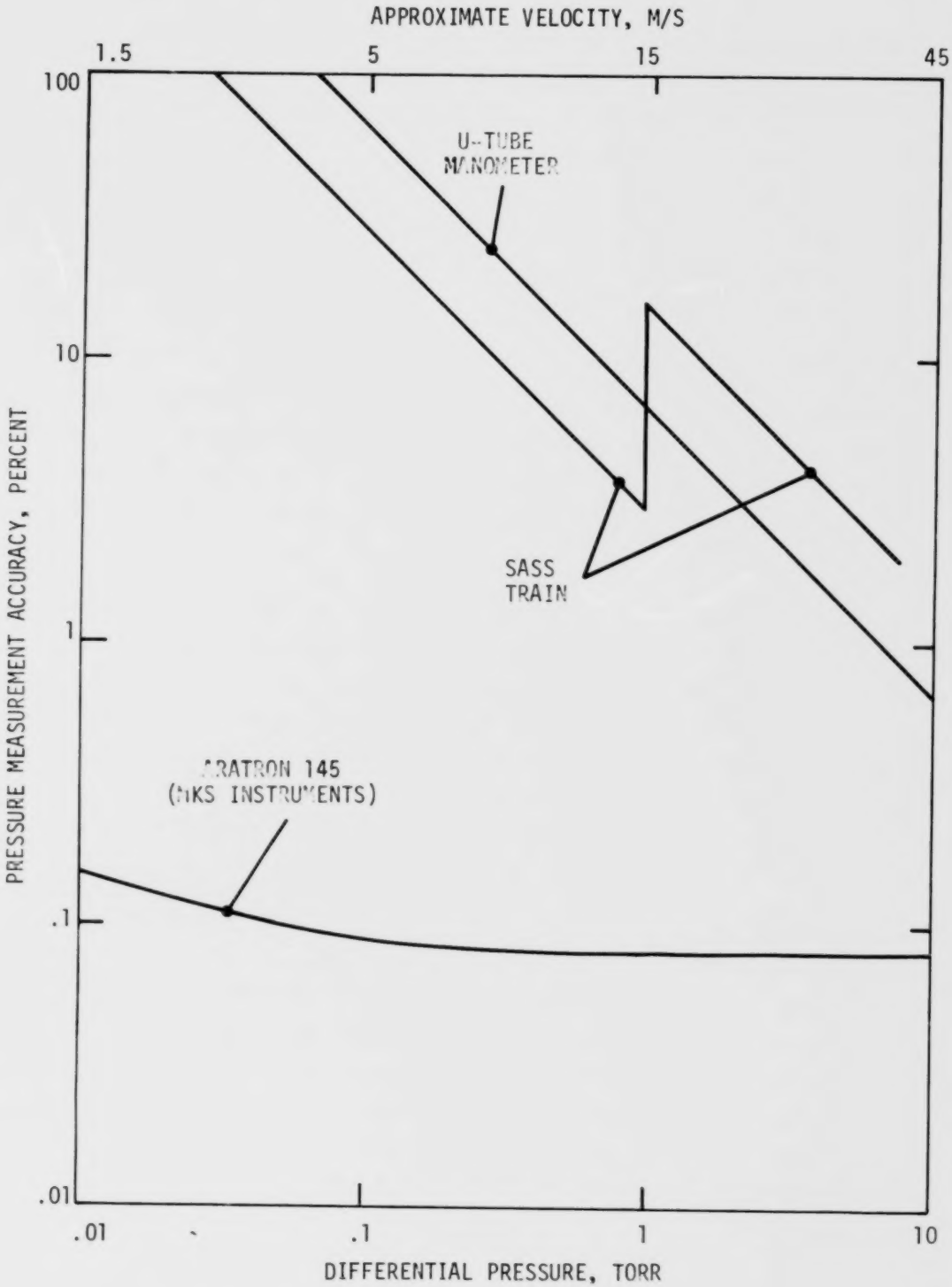

Figure B-2. Differential pressure measurement accuracy of various devices

steady state entities, which makes flow visualization techniques such as smoke filaments in air flow or dye filaments in liquid flow viable. In a turbulent stream, streamlines exist instantaneously only -- the streamline pattern varies greatly from millisecond to millisecond. These changes are typically not small. In a fully developed turbu pipe flow, the turbulence is structured such that turbulent eddies tend to move downstream as units (Reference B-4). Experimental studies have shown that the size of these turbulent eddies is about 7% of the pipe diameter (Reference B-5). In a fully developed turbulent pipe flow, the velocity component parallel to the sample probe axis can be expected to fluctuate over about a ±10% (of axial flow velocity) range, with similar fluctuations in the angle of the velocity vector at the probe tip (Reference B-6). For operation near an elbow or other large disturbance, these fluctuations will be even worse due to the larger local scale of turbulence caused by flow detachment.

What this all means is that in real life, isokinetic sampling is a type of averaging process. In all cases, we can expect that the stream turbulence scale will be large with respect to the sampling orifice, so there is no easy way to get around the turbulence problem. The primary reason for the above commentary is to illustrate that while isokinetic sampling can be performed in a good laminar flow wind tunnel, it can only be approximated in actual process streams.

Watson's expression for isokinetic sampling errors (Refereces B-7 and B-8), the experimental verification for which was obtained in a low turbulence wind tunnel, is as follows:

$$C_m = C_A \frac{U_G}{U_m} \left\{ 1 + f(8) \left[\left(\frac{U_m}{U_G} \right)^{\frac{1}{2}} - 1 \right] \right\}^2 \qquad \text{(B-1)}$$

where

C_m = aerosol concentration inside probe entry, g/cm^3

C_A = true aerosol concentration in the stream ahead of the probe, g/cm^3

U_G = true gas velocity ahead of the probe, cm/s

U_m = mean velocity at probe inlet, cm/s

$$\beta = \frac{D_p \rho_p U_G}{18\mu D_s}$$

f = empirical functional relationship

D_p = particle diameter, cm

ρ_p = particle density, g/cm^3

μ = gas viscosity, poise

D_s = sample probe orifice diameter, cm

Equation (B-1) is plotted in Figure B-3 for different values of the various parameters. In practice, the plot says that anisokinetic sampling does not lead to concentration errors as the particles become very small, while in the limit of large, dense particles, the concentration error is inversely proportional to the velocity error, i.e.

$$\frac{C_m}{C_A} \rightarrow \frac{U_G}{U_m} \quad \text{for large, dense particles.}$$

In normal practice, the stream velocity is measured with a pitot probe and the sampling velocity U_m is set equal to the measured velocity. For this mode of operation, the measured aerosol mass flux at the sampling point becomes (ignoring α for the moment)

$$\left(\frac{d\dot{m}_A}{dA}\right) = C_m U_m \qquad \text{(B-2)}$$

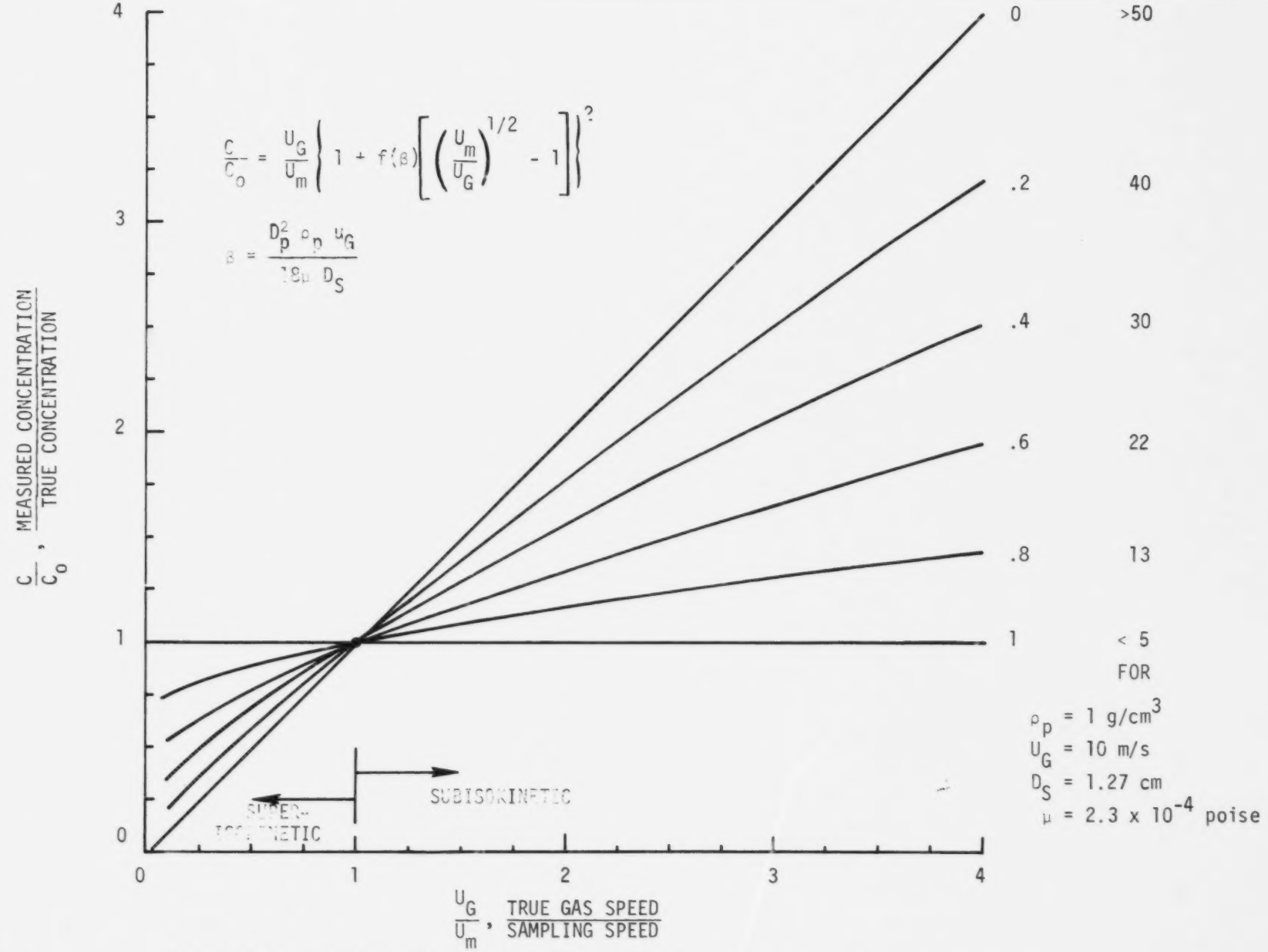

Figure B-3. Particulate measured concentration error as a function of sampling velocity (Anisokinetic) error for various aerosol conditions (from Watson, Reference B-7)

while the true mass flux is

$$\left(\frac{d\dot{m}_A}{dA}\right) = C_A U_G \qquad \text{(B-3)}$$

applying the small and large particle limits of equation (B-1), we obtain

$$0 \leq \left| \left(\frac{d\dot{m}_A}{d_A}\right)_{meas} - \left(\frac{d\dot{m}_A}{d_A}\right)_{true} \right| \leq \left| C_A \left(U_m - U_G\right) \right| \qquad \text{(B-4)}$$

where zero error occurs for the case of large particles, while non-zero error occurs for very small particles and is in fact solely a velocity measurement error unrelated to the sampling process. In other words, as long as sampling velocity and measured velocity are kept identical, anisokinetic sampling of large particles compensates for velocity measurement errors, while anisokinetic sampling of small particles does not lead to a concentration measurement error. For total particulate measurement errors, then, we may make the following statement:

> Particle mass emission errors at a point will not be larger than errors in the measured stream velocity as long as the sample velocity is maintained equal to the measured velocity and the sampling probe is properly aligned with the stream.

It must be noted that the above statement applies only to particle mass emission and only at individual points. The relationship between point measurements and the total emission is related to stratification, which is treated below. The important point is that isokinetic errors and velocity measurement errors are compensating rather than additive.

Concentration measurement errors due to anisokinetic sampling depend, of course, on all the factors shown in equation B-1. Reference B-7 recommends the values shown in Table B-2 "for the size distribution of dusts encountered in practice". The following general rule is also

Table B-2. Effect of Departure from Isokinetic Conditions on Sample Concentrations (from Reference B-7)

$\frac{u_G}{u_S}$	$\frac{C}{C_o}$	
	RANGE	TYPICAL VALUE
0.6	0.75-0.90	0.85
0.8	0.85-0.95	0.90
1.2	1.05-1.20	1.10
1.4	1.10-1.40	1.20
1.6	1.15-1.16	1.30
1.8	1.20-1.80	1.40

recommended in Reference B-7:

> "Isokinetic sampling is unnecessary for smoke and fumes which are not admixed with particulate matter over 5μ in size."

It is clear that for purposes of error analysis, the term $\sigma_{\dot{m}_A}$ should be coupled with the velocity error terms due to the compensating aspects. Aside from the traditional isokinetic sampling aspects, we must also be concerned with misalignment of the sampling probe with respect to the local stream direction. As explained above, the flow direction goes through instantaneous changes, but these average out reasonably over the sampling period in most cases when the volumetric flow rate stays constant. Any misalignment of the sampling probe reduces the number of large particles (> 5μ) collected, while collection of small particles is affected little, if at all. Failure of the sampling team to align the sampling probe parallel to the duct or stack axis within two or three degrees constitutes a mistake rather than a random error. Non-alignment of the flow itself with the stack axis must generally be considered a random error since the sampling team will usually not have the instruments to properly determine flow direction. The best way to avoid flow angularity is to use the standard "eight diameters downstream and two diameters upstream of a disturbance" approach when possible. In stacks, the flow will tend to be axially aligned within a few diameters from the breaching except in the case of swirling (cyclonic) flow, which can persist much longer. Reference B-9 makes the following statements about such flows:

> "....severe cyclonic motion has not been observed in large power plant stacks."

Unfortunately, it is also concluded that

> "Little qualitative data is available defining flow angularity in large (>100 MW) power plant stacks."

To summarize the above commentary and relate it to actual hardware, it can be said that the major error sources for collected

particulate mass are non-isokinetic sampling, probe/flow misalignment, and sample gain or loss within the probe. For the SASS train, non-isokinetic sampling occurs because the sample flow rate must be held constant. Since a sampling crew will have a limited number of inlet nozzle sizes, there will be a differential between the nozzle inlet velocity and the local stream velocity. In addition, this configuration does not allow for adjustments in sampling rate during a run to compensate for any free stream velocity changes. In an optimum train, the sampling velocity would be continually adjusted so that it matched the measured stream velocity. The discussion associated with equation (B-4) says that if this can be accomplished, errors in isokinetic sampling tend to compensate for velocity measurement errors. In the turbulent flows which occur in real life, it will not be possible to match the sample flow rate to the measured velocity, since the latter will fluctuate more rapidly than the sample flow can be adjusted.

The error estimates in Table 3 of the text for σ_{m_A} are based on known SASS train characteristics, accuracies (velocity measurement in particular) of other commercially available hardware, and estimates of actual flow conditions to be encountered at the three types of designated sampling locations. For the SASS train, the greatest source of error is the anisokinetic error, while misalignment will be the largest source for the hypothetical "maximum accuracy train". The basic difference between the two trains would be greater velocity measurement accuracy and continuously variable sampling velocity for the "maximum accuracy train". Errors are predicted highest at a control device inlet due to the size distribution (maximum number of large particles) and anticipated flow angularities. (See Reference B-9 for compilations of control device inlet and outlet size distributions.) Errors will be at a minimum in a stack due to smaller flow angularities and removal of large particles in a control device.

4. Mapping (Handling of Stratification)

There are three major difficulties involved in dealing with stratification problems: (1) The stratification level itself is often very large, which leads to large errors, especially for single point sampling. (2) More background data are needed to assess the severity of the problem. (3) There is a shortage of methodology for sampling techniques in stratified streams. The first point is illustrated in Table B-3, taken from Reference B-10. Particulate mass concentration maps were taken for the four cases listed (the ESP data is true field data). Large variations from the mean concentration were observed in each case. Of particular interest is the ESP data, which shows that the device was definitely a source of stratification. The variations shown in Table B-3 clearly indicate that single point sampling is likely to result in large mapping errors.

There is no question that much more stratification data exist than were examined for this report. As much data was examined as could be obtained within the scope of work. Comparison data between single point impactor sampling and multiple point Method 5 type sampling is shown in Tables B-4 and B-5. The data were obtained from References B-11 and B-12, respectively, supplied by Joe McCain of Southern Research Institute. The data in Table B-4 represent a summary of many runs. The "minimum" and "maximum" errors are the best and worst correlations obtained among the individual runs, while the "nominal" error was the average error for all runs in the category. The data in Table B-5 are for individual runs. A very important item to keep in mind when examining these data is that entirely different types of sampling trains were used to obtain the single point (impactors were used here) and multiple point (Method 5 type train) data. This makes it impossible to isolate the mapping error due to single point sampling. Data type and quality are discussed further in Appendix C. What is needed is more mapping data obtained with a single

Table B-3. Summary of Particulate Mapping Data from Fluidyne "Particulate Sampling Strategies" Report (Reference B-9)

DESCRIPTION	CENTER POINT CONCENTRATION ERROR, %	VARIATION IN SAMPLE PLANE FROM MEAN CONCENTRATION, %	
		LOW	HIGH
Downstream of ESP	-16	-74	+268
Upstream of ESP	+13.5	-35	+ 30
"Theoretical" distribution downstream of ESP	-62.8	-63	+160
Laboratory scale model flow	- 2.33	-19	+117

Table B-4. Summary of Comparison of Single Point Impactor Data Versus Method 5 Traverse at an ESP Outlet, from Southern Research Institute EPRI Report (Reference B-11)

OPERATING MODE*	SINGLE POINT ERROR USING METHOD 5 TRAVERSE AS A REFERENCE, %		
	MINIMUM	NOMINAL	MAXIMUM
With SO_3	- 5	-33	-61
Without SO_3	-68	-75	-94

*SO_3 injection was used as a mechanism to minimize re-entrainment due to rapping. Lower loading and less stratification occurred with SO_3 injection.

Table B-5. Grain Loading Errors for Single Point Impactor Sampling, Using Conventional (ASME, EPA) Mass Train Traverse Measurement As Reference Data (Data taken from Reference B-12)

SITE	RUN NO.	SINGLE POINT MASS LOADING ERROR, %
1	1	+711
	2	+256
	3	+227
	4	+ 26
	5	+ 6
	6	+ 5
	7	+131
2	1	- 34
	2	- 35
	3	- 43
3	1	- 38
	2	- 19
	3	- 50
4	1	- 6
	2	- 45
	3	- 48
	4	- 50

Sites: At all sites, location was control device outlet

1 - Coal fired power plant
2 - Coal fired power plant
3 - Electric arc smelting furnace
4 - Coal fired power plant

instrument, as was done to obtain the data summarized in Table B-3.

The data in Table B-4 are a good illustration of the need for better sampling methodology. The impactor sampling point used was not representative of the distribution in the stream, leading to errors of as high as a factor of 16. The Level 1 approach of using a point of average velocity as the sampling point is a step in the right direction since such a point is less likely than most to result in misalignment errors, will not be in a recirculation region, and at least will be representative of total mass transport. For stack sampling, it may be the case that further refinements to this approach will not be needed. For sampling at a control device outlet, however, Table B-4 points out the need for taking the device's characteristics into account in the selection of a sampling point or points.

Particulate stratification originates where the particles originate, e.g. in the furnace of a coal fired power plant. Stratification can be made worse by in-leakage of air. Removal devices can make stratification either more or less severe, according to their operating characterisitics. Changes in ducting shape and direction simultaneously promote convective mixing (reduces stratification) and inertial separation (increases stratification). The combination of desired accuracy and stratification provides the answer to the question, "To single point or not to single point?". This question has been studied more extensively for flow measurement and gas sampling than for particulate sampling, but should apply to that case as well. Reference B-13, which is basically a summarization of the velocity measurement data in Reference B-10, and Reference B-14 conclude that the 2σ mapping error of a 12-to-16 point traverse is about a factor of five less than that for a single point measurement for volumetric flow (References B-12 and B-13) and gas composition (Reference B-13). As the mean particle size becomes small ($<5\mu$), particulate stratification is almost identical in mechanism to gas stratification because of

the dominance of convective mixing in both cases. In Reference B-15, the average 2σ single point gas composition mapping error was found to be ±15%. There is no reason to believe the single point particulate sampling mapping error would be better than this figure, and indeed will be much worse in most cases. The data which have been examined are not sufficient to establish good bounds for single point particulate sampling. Accumulated data for volumetric flow and gas composition lead to the conclusion that a properly performed traverse using about 16 points will result in σ_{ME} not being the major source of system error.

The single point mapping error estimates in Table 4 in the text were derived from Tables B-3 and B-5, taking into account the difference in trains in the latter. The traverse error estimates were obtained by comparing the maps in Reference B-10 with gas composition maps in Reference B-14. The mapping error itself is independent of the sampling equipment used. The mapping error estimates must at present be considered the least firm of all the error estimates in the text, which is unfortunate since the mapping error is by far the largest error in the system for single point sampling. The need for more data to "firm up" the estimates is discussed in Appendix C.

APPENDIX B. REFERENCES

B-1. "Continuous Measurement of Total Gas Flowrate from Stationary Sources," EPA-650/2-75-020, Brooks, et al., February 1975.

B-2. The Measurement of Air Flow, E. Ower and R. C. Pankhurst; Pergamon Press, 1966.

B-3. "Recent Environmental Assessment Studies," (Draft Copy), Monsanto Research Corporation, November 1976.

B-4. Boundary Layer Theory, H. Schlichting; McGraw-Hill Book Company, 1968.

B-5. "Correlation Measurements in a Turbulent Flow Through a Pipe," G. I. Taylor, Proc. Roy. Soc. A 157, 537-546,1936.

B-6. "The Structure of Turbulence in Fully Developed Pipe Flow," J. Laufer, NACA TN 2954, 1953.

B-7. Air Pollution, Volume II, A. Stern, ed., Academic Press, 1968.

B-8. H. H. Watson, Am. Ind. Hyg. Assoc. Quart. 15, 21, 1954.

B-9. "Particulate Sampling Strategies for Large Power Plants Including Non-uniform Flow," EPA-600/2-76-170, Hanson, et al., June 1976.

B-10. "Fine Particle Emissions Information System: Summary Report (Summer 1976)," EPA-600/2-76-174, Schrag and Rao, June 1976.

B-11. "Proceedings on the Workshop on Sampling, Analysis, and Monitoring of Stack Emissions," EPRI SR-41, Southern Research Institute, April 1976.

B-12. "Particulate Sizing Techniques for Control Device Evaluation," EPA-650/2-74-102-a, Smith, et al., August, 1975.

B-13. "The Number of Sampling Points Needed for Representative Source Sampling," K. T. Knapp, paper presented at Fourth National Conference on Energy and Environment, October 1976.

B-14. "Flow and Gas Sampling Manual," EPA-600/2-76-203, Brooks and Williams, July 1976.

B-15. "Continuous Measurement of Gas Composition from Stationary Sources," EPA-600/2-75-012, Brooks, et al., July 1975.

APPENDIX C. COMMENTS ON DATA AND ERROR ANALYSES

As stated in the text, the error analysis performed was identical in form to that in Reference C-1. The explicit portion of the error analysis is similar in concept to that in Reference C-2. A nominal 2σ system error of ±16% was obtained for a total particulate mass measurement involving a traverse. This estimate is similar to those for traverses in Table 5. A more encompassing error discussion is given in Reference C-3, and treats both explicit and non-explicit error sources. However, error bounds were not well established in this analysis.

The nature of the measurement for total particulate mass dictates that two distinct groups of information must be consulted to determine system accuracy - sampling hardware characteristics and source characteristics. For parameters such as temperature and static pressure, it is normally the case that measurement accuracy can be determined from the hardware alone. The accuracy of parameters such as velocity and collected particulate mass usually depend on both hardware and source characteristics. At the other extreme, mapping errors depend only on source characteristics. The great variety of source characteristics makes it impossible to perform a system error analysis and arrive at a single number for system accuracy, just as it would be impossible to arrive at a single number result for an analysis of a variety of sampling trains. The final selected approach of looking at two types of trains in three generalized sampling situations was intended to show the relative impact of hardware and source on system accuracy.

Most error analysis work deals with identification and evaluation of specific error sources. The interrelationship of hardware and source characteristics for particulate sampling necessarily complicates isolation of errors. During the present study, this problem caused the most difficulty in evaluation of the error terms σ_{m_A} and σ_{ME}. As was mentioned in Appendix B, evaluation of anisokinetic sampling errors has traditionally been performed in laminar flow wind tunnels. The turbulent, unsteady flows

in process streams make it difficult to adapt laminar flow data to the real life case. That approach has been used of necessity, however, since it has not been possible to obtain high accuracy reference data needed for an error assessment in the field.

The bulk of the mapping data summarized in Appendix B has the problem that the single point data was obtained with significantly different hardware than the traverse data. This makes it impossible to separate the hardware error from the mapping error. There is no question that mapping data of the type desired (a concentration map obtained with a single probe) is difficult, time consuming, and costly to obtain. In this instance, it is felt that the effort would be justified due to the magnitude of mapping errors. In addition to supporting error analysis work, the same data would be essential to the development of methods for obtaining representative samples through judicious selection of a single sampling point or a small number of sampling points.

The functional purpose of a system error analysis, in addition to producing the bottom line number for total system accuracy, is to determine the relative importance of the individual error sources. This information tells the worker which hardware components in a given system should be upgraded to achieve a desired accuracy, and which components may be replaced with less expensive, less accurate ones without significantly altering the system accuracy. The same is true of sampling procedures, the most obvious example being selection of single or multiple point sampling techniques to achieve a given accuracy. A proper error analysis is thus the technical foundation for optimum allocation of funds and manpower to achieve sampling data of appropriate quality for the tasks at hand.

APPENDIX C. REFERENCES

C-1. "Flow and Gas Sampling Manual," EPA-600/2-76-203, Brooks and Williams, July 1976.

C-2. Industrial Source Sampling, Brenchley, Turley, and Yarmac, Ann Arbor Science Publishers, Inc., 1973.

C-3. "A Manual of Electrostatic Precipitator Technology, Part I - Fundamentals," NTIS PB-196 380, Oglesby, et al., August 1970